



Rogue Mantle Helium and Neon

Francis Albarède, *et al.*

Science **319**, 943 (2008);

DOI: 10.1126/science.1150060

The following resources related to this article are available online at www.sciencemag.org (this information is current as of February 18, 2008):

Updated information and services, including high-resolution figures, can be found in the online version of this article at:

<http://www.sciencemag.org/cgi/content/full/319/5865/943>

This article **cites 31 articles**, 3 of which can be accessed for free:

<http://www.sciencemag.org/cgi/content/full/319/5865/943#otherarticles>

This article appears in the following **subject collections**:

Geochemistry, Geophysics

http://www.sciencemag.org/cgi/collection/geochem_phys

Information about obtaining **reprints** of this article or about obtaining **permission to reproduce this article** in whole or in part can be found at:

<http://www.sciencemag.org/about/permissions.dtl>

with that of BPL carbon, ZIFs have higher selectivity (Table 2). In terms of storage capacity and selectivity to CO₂, ZIF-69 and 70 outperform BPL carbon and all the other ZIFs that we have examined.

References and Notes

- D. E. Akporiaye, I. M. Dahl, A. Karlsson, R. Wendelbo, *Angew. Chem. Int. Ed.* **37**, 609 (1998).
- J. Klein, C. W. Lehmann, H. W. Schmidt, W. F. Maier, *Angew. Chem. Int. Ed.* **37**, 3369 (1998).
- K. Choi, D. Gardner, N. Hilbrandt, T. Bein, *Angew. Chem. Int. Ed.* **38**, 2891 (1999).
- R. Lai, B. S. Kang, G. R. Gavalas, *Angew. Chem. Int. Ed.* **40**, 408 (2001).
- M. Forster, N. Stock, A. K. Cheetham, *Angew. Chem. Int. Ed.* **44**, 7608 (2005).
- N. Stock, T. Bein, *Angew. Chem. Int. Ed.* **43**, 749 (2004).
- A. Corma, M. J. Díaz-Cabanas, J. L. Jordá, C. Martínez, M. Moliner, *Nature* **443**, 842 (2006).
- K. S. Park *et al.*, *Proc. Natl. Acad. Sci. U.S.A.* **103**, 10186 (2006).
- H. Hayashi, A. P. Côté, H. Furukawa, M. O'Keeffe, O. M. Yaghi, *Nat. Mater.* **6**, 501 (2007).
- R. Lehnert, F. Seel, *Z. Anorg. Allg. Chem.* **464**, 187 (1980).
- S. J. Rettig, V. Sánchez, A. Storr, R. C. Thompson, J. Trotter, *J. Chem. Soc. Dalton Trans.* **2000**, 3931 (2000).
- Y. Liu, V. Ch. Kravtsov, R. Larsena, M. Eddaoudi, *Chem. Commun.* **2006**, 1488 (2006).
- J.-P. Zhang, X.-M. Chen, *Chem. Commun.* **2006**, 1689 (2006).
- Y.-Q. Tian *et al.*, *Chem. Eur. J.* **13**, 4146 (2007).
- C. Baerlocher, L. B. McCusker, Database of Zeolite Structures (www.iza-structure.org/databases).
- M. E. Davis, *Nature* **417**, 813 (2002).
- The isolation of the sample array is accomplished in parallel by sonication and transfer in a custom-designed shallow metal plate, which allows the presence of a small amount of solvent during the PXRD data collection. The samples were then analyzed by a Bruker D8 DISCOVER high-throughput PXRD instrument with a movable horizontal x-y stage for automated analysis and an image plate detector system. The data collection time was 3 to 6 min per sample. The PXRD patterns thus collected were compared against an in-house library of PXRD patterns of known ZIFs and other network-type materials.
- Reticular Chemistry Structure Resource (<http://rcsr.anu.edu.au>).
- O. Delgado-Friedrichs, M. O'Keeffe, O. M. Yaghi, *Acta Crystallogr. A* **59**, 22 (2003).
- V. A. Blatov, O. Delgado-Friedrichs, M. O'Keeffe, D. M. Proserpio, *Acta Crystallogr.* **A63**, 418 (2007).
- N. L. Rosi *et al.*, *J. Am. Chem. Soc.* **127**, 1504 (2005).
- F. Rouquerol, J. Rouquerol, K. Sing, *Adsorption by Powders and Porous Solids* (Academic Press, London, 1999).
- S. Sircar, T. C. Golden, M. B. Rao, *Carbon* **34**, 1 (1996).
- The work was supported by Badische Anilin und Soda Fabrik (BASF) Ludwigshafen for synthesis, the U.S. Department of Energy (DEFG0206ER15813) for adsorption and separations studies, and the U.S. Department of Defense (W911NF-061-0405) for equipment used for breakthrough experiments. Crystallographic data for the structures reported in this paper have been deposited with the Cambridge Crystallographic Data Centre under reference numbers CCDC 671067 to 671089. These data can be obtained free of charge via www.ccdc.cam.ac.uk/conts/retrieving.html (or from the Cambridge Crystallographic Data Centre, 12 Union Road, Cambridge CB2 1EZ, UK).

Supporting Online Material

www.sciencemag.org/cgi/content/full/319/5865/939/DC1
SOM Text S1 to S5
Figs. S1 to S86
Tables S1 to S23

2 November 2007; accepted 3 January 2008
10.1126/science.1152516

Rogue Mantle Helium and Neon

Francis Albarède

The canonical model of helium isotope geochemistry describes the lower mantle as undegassed, but this view conflicts with evidence of recycled material in the source of ocean island basalts. Because mantle helium is efficiently extracted by magmatic activity, it cannot remain in fertile mantle rocks for long periods of time. Here, I suggest that helium with high ³He/⁴He ratios, as well as neon rich in the solar component, diffused early in Earth's history from low-melting-point primordial material into residual refractory "reservoir" rocks, such as dunites. The difference in ³He/⁴He ratios of ocean-island and mid-ocean ridge basalts and the preservation of solar neon are ascribed to the reservoir rocks being stretched and tapped to different extents during melting.

Helium-4 is a radiogenic nuclide produced in Earth and other planetary bodies by the alpha decay of uranium and thorium. In contrast, most of the ³He present is a regular stable nuclide. The relative abundances of the two isotopes in oceanic basalts therefore reflect the evolution of the parent/daughter ratio (U+Th)/He. These three elements are strongly incompatible (i.e., excluded from the structure of the major silicate materials), but one of them (He) is markedly affected by outgassing. Helium preferentially partitions not only into any gas phase present, but also into liquid during melting (1). Contribution from primitive undegassed mantle gives basalts very low ⁴He/³He ratios. The canonical model holds that high ⁴He/³He ratios characterize high (U+Th)/He mantle sources, such as the mantle underneath mid-ocean ridges, which were degassed during successive melting events. If He is less incompatible than both Th and U, however, these

low ³He/⁴He regions could instead signal mantle that was depleted in incompatible elements upon melting (1, 2). However, the abundances of rare gases differ between these two models, being high for undegassed mantle and very low for residual mantle.

For historical reasons, He isotopic compositions are reported upside down as R/R_{atm}, where R denotes the ³He/⁴He ratio and the subscript signals the normalization to the atmospheric ratio. More than 30 years of observations have shown that mid-ocean ridge basalts (MORBs) are characterized by a narrow range of ³He/⁴He ratios clustering about 8 R_{atm}, whereas values in excess of 20 R_{atm} are found nearly exclusively in ocean-island basalts (OIBs) (3–6). These data support the idea that MORBs are derived from parts of Earth's mantle that are significantly more degassed than the source of OIBs (5, 7, 8). If pushed to the extreme, the assertion that OIBs are tapping a deep, largely undegassed part of the mantle implies that the lower mantle is pristine and that mantle convection takes place as separate layers (9, 10).

This canonical view, however, conflicts with several critical observations on OIBs. Nearly every isotopic system involving lithophile elements—notably ⁸⁷Rb-⁸⁷Sr, ¹⁴⁷Sm-¹⁴³Nd, ¹⁷⁶Lu-¹⁷⁶Hf, and ¹⁸⁷Re-¹⁸⁷Os—indicates that the mantle source of MORB and OIB is de-

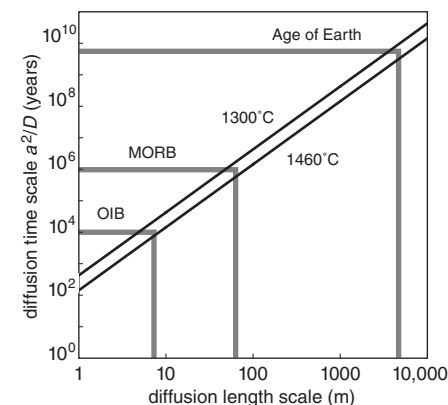


Fig. 1. Relationship between the time and length scales of diffusion in olivine, using the data of Shuster *et al.* (20) at two different temperatures. The two isotopes of He have comparable diffusion rates. At a temperature of 1460°C, He and Ne have the same diffusivity in quartz, which suggests that He and Ne diffusivity at mantle temperatures in mantle minerals may not be very different. The set of values labeled "Age of Earth" show that over the geological ages, He and Ne may have moved by diffusion over distances in excess of several kilometers. Assuming that melting takes place in the uppermost 100 km and an upwelling velocity of 10 m year⁻¹ beneath OIBs and 10 cm year⁻¹ beneath MORBs gives time scales for diffusion; the corresponding distances of diffusion relevant to melt extraction for MORB and OIB can be read from the curve (see text).

pleted in fertile components with respect to chondrites. Even stronger evidence against primitive mantle is the surprisingly large range of $\delta^{18}\text{O}$ values in Hawaiian basalts, which attest to the OIB source holding a component that went through low-temperature alteration, and the correlation of $^{187}\text{Os}/^{186}\text{Os}$ with $\delta^{18}\text{O}$ (11). The correlation between Hf and Pb isotopes further indicates the presence of pelagic sediments in the source of the Hawaiian plume (12). These observations raise the question of how Hawaiian basalts, which carry the embodiment of a primordial gas signature, at the same time can provide such strong evidence of surface material recycling. They are not explained by geodynamic models in which high $^3\text{He}/^4\text{He}$ ratios in oceanic basalts reflect a contribution from blobs of primordial material drifting in the mantle flow field (13).

A solution to this conundrum may lie in an analogy with oil genesis: ^3He is unlikely to escape melting events and magmatic outgassing for billions of years of whole-mantle convection if it resides in fertile, low-melting-point rocks, but large quantities may remain buried at depth if He migrates into refractory reservoir rocks. Because there can be no free gas phase percolating at pressures in excess of olivine carbonation at ~ 3 GPa (14), He must be largely redistributed by diffusion. Given the lack of isotopic evidence for the persistence of large swaths of primordial mantle, the dual fate of He must consist in being hosted either by fertile material, from

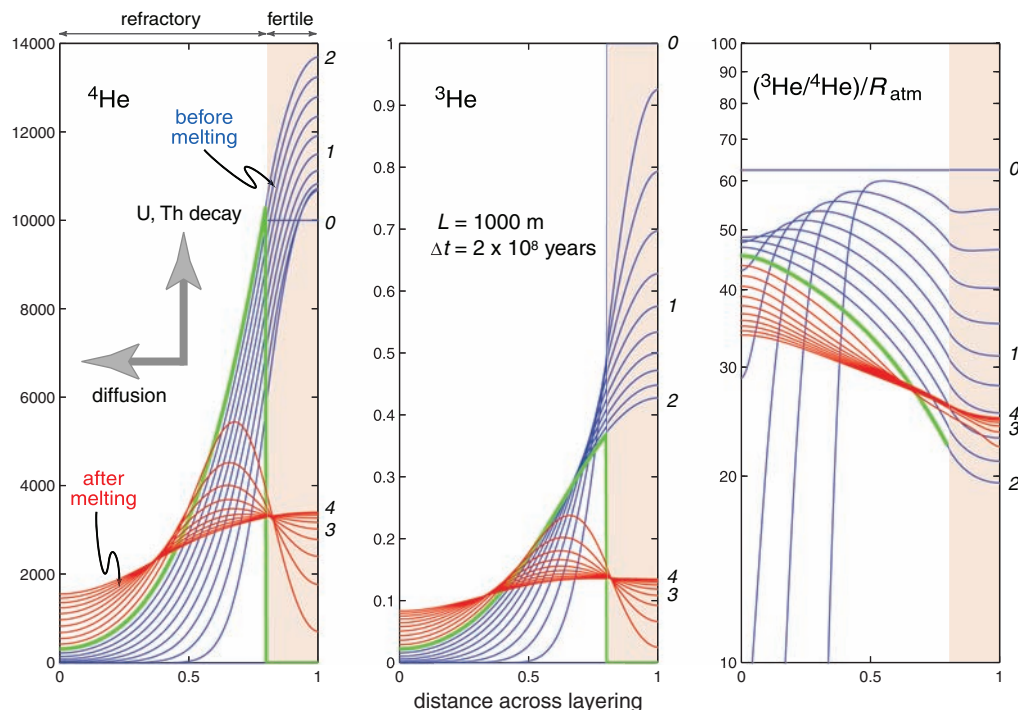
which it is eventually extracted to the atmosphere upon decompressional melting, or by refractory rocks.

Very different gradients of ^3He and ^4He across the system favor the increase of $^3\text{He}/^4\text{He}$ in refractory rocks. Helium-3 was originally present in frozen He-rich material evolved from the early magma ocean, such as pyroxenites and fertile peridotite. Throughout Earth's history, ^3He migrated deeper and deeper into thick layers of He-poor refractory rocks, first in cumulates of the magma ocean (15, 16) and subsequently in olivine-rich dunites and harzburgites formed under mid-ocean ridges (17). Changes in the mineralogy of the alternating layers with depth are not relevant as long as melt is not present. The persistence of high $^3\text{He}/^4\text{He}$ mantle regions therefore boils down to two simple questions: (i) how He migrated into deep-seated refractory reservoirs in the first place, and (ii) how it was extracted from its reservoir upon melting. The "helium-recharged depleted mantle" model of Ellam and Stuart (18) assumes conservative mixing between depleted and undegassed mantle. Inefficient He extraction does not result from the persistence of abundant gas cavities during shallow melting (19), because bubbles would need to hold back exceedingly large amounts of rare gases. The case for He-poor, high- $^3\text{He}/^4\text{He}$ residues implied by the assumption that He is slightly less incompatible than U and Th during melting (1) is, by contrast, fully compatible with the present model.

Figure 1 shows the overall scaling of He diffusion in mantle rocks. The He volume diffusivity in olivine was recently redetermined, and ^3He and ^4He were shown to diffuse at comparable rates (20). Because of the exponential dependence of diffusivity on the inverse of temperature, the results are virtually independent of the choice of a particular mantle temperature. At 1300° to 1400°C , it only takes He $\sim 10^4$ years to migrate over ~ 10 m and 10^8 years to cover 1 km.

A quantitative model illustrates how rogue mantle rare gases move around (Fig. 2). I assume that mantle material consists of alternating thin layers of low-melting-point rocks, either primordial fertile peridotite or pyroxenites, embedded in thicker layers of refractory dunite and harzburgite (21). The model assumes radiogenic ^4He ingrowth from U and Th. Initially, ^3He , U and Th are much more concentrated in the fertile layers than in residual rocks. For simplicity, I assume that the mantle is homogeneously striped, so that, by symmetry, a no-flux condition applies at the center of both the pyroxenite and dunite layers. The model described in Fig. 2 postulates that ^3He initially hosted in a 200-m-thick layer of primordial material diffuses into the 800-m-thick ^3He -poor refractory layer for 2×10^9 years. At this point, a small fraction of melt is removed from the fertile layer entraining its He, U, and Th, possibly during one of the mantle events suggested by Parman (22). I further assume that either the residuum of the fertile layer is preserved or that it is replaced

Fig. 2. A two-stage history of He in the marble-cake mantle made of fertile (e.g., U- and Th-rich "pyroxenite" in beige) and refractory (e.g., U- and Th-poor "dunite" in green) rocks. The figure represents He diffusion over 4×10^9 years, with a double-layer geometry and a melting event at 2×10^9 years ago. The curves show He profiles across the system every 2×10^8 years; the labels in italic along the right edges indicate numbers of years ($\times 10^9$) before the present. The thicknesses of the refractory and the fertile layers are 800 and 200 m, respectively ($L = 1000$ m). The He diffusion coefficient is taken to be $10^{-12} \text{ m}^2 \text{ s}^{-1}$ (20). Helium-3 concentrations are normalized to their initial value in the fertile layer. The initial $^4\text{He}/^3\text{He}$ ratio of Earth is taken as 8000. Fertile material has a $^{238}\text{U}/^3\text{He}$ ratio of 15,000 before melting and 500 after melting. $^3\text{He}/^4\text{He}$ ratios are normalized to the modern atmospheric ratio $R_{\text{atm}} = 1.4 \times 10^{-6}$. It is assumed that ^3He is introduced at $t = 0$ into the system with the fertile layer before significant ingrowth of radiogenic ^4He . A core of helium with a high $^3\text{He}/^4\text{He}$ ratio moves into the dunite (right panel). The episode of melting (green curves) removes helium with a low $^3\text{He}/^4\text{He}$ ratio from the fertile layer and therefore helps to maintain isotopic gradients across the system. After melting (red curves), helium



with a high $^3\text{He}/^4\text{He}$ ratio diffuses back from the dunite into the still fertile, but no longer pristine and undegassed, pyroxenite layer. Refractory He-, U-, and Th-poor dunite therefore acts as a long-term reservoir for He and Ne.

by an equivalent layer of subducted pyroxenite, which is a simple way of maintaining the double-layer structure. The diffusion equations were solved using an implicit finite-difference scheme. In the absence of relevant data, I assume that the high- and low-pressure forms of these rocks behave identically with respect to He diffusion.

In the interval from 2×10^9 years ago to the present (in blue in Fig. 2), significant radiogenic ^4He has not yet accumulated in the fertile layer, and the core of helium diffusing into the U- and Th-poor refractory layer therefore has a high $^3\text{He}/^4\text{He}$ ratio. At 2×10^9 years ago, the episode of melting (in green) removes helium with a low $^3\text{He}/^4\text{He}$ ratio from the fertile layer, which thereby helps maintain isotopic gradients across the system. The interval from 2×10^9 to 4×10^9 years ago (in red) shows how the fertile layer, regardless of its origin, is replenished in helium with a high $^3\text{He}/^4\text{He}$ ratio by the refractory layer.

The contrast between MORB and OIB sources can thus be accounted for simply by different proportions of high- $^3\text{He}/^4\text{He}$ reservoir rocks being unaffected by the melt extraction process. Assuming for simplicity that melts begin forming over the uppermost 100 km with an upwelling rate of 10 m year^{-1} beneath OIBs and 10 cm year^{-1} beneath mid-ocean ridges, the characteristic times of melt extraction in these two environments are 10^4 years and 10^6 years, respectively, and the maximum thicknesses of refractory layers contributing their He to the magmas are 10 m and 100 m, respectively (Fig. 1). For OIBs, both the existence of high- $^3\text{He}/^4\text{He}$ regions and the coexistence of high- and low- $^3\text{He}/^4\text{He}$ magmas are adequately explained by the variable stretching of refractory layers present in the upwelling region. Because of temperature-dependent viscosity, shear is maximum along the edge of conduits: Outgassing of large lumps of residual material down to a dimension of $<100 \text{ m}$ should allow for a quick transfer of the high- $^3\text{He}/^4\text{He}$ signature to their surroundings, including the fertile components, which eventually melt and form OIBs. The highest $^3\text{He}/^4\text{He}$ ratios (>30) are found in the infant volcano of Loihi on the southeastern flank of Hawaii (8) and in the northwesternmost lavas of Selaldalur in Iceland (23). Pyroxenite layers not brought into contact with such initially large lumps of residues, in contrast, could be parent to low- $^3\text{He}/^4\text{He}$ basalts, which provides an alternative to the interpretation that the source of low- $^3\text{He}/^4\text{He}$ hot spots, such as Gough or Tristan, is dominated by recycled crustal material (8).

The flow regime beneath mid-ocean ridges is expected to be laminar, with weaker velocity gradients and only mild shearing. The distribution of the spacing between alternating values of Hf isotopes along the Southeast Indian Ridge implies an exponential distribution of layer thicknesses (24). The $^3\text{He}/^4\text{He}$ ratio of MORB therefore represents an aver-

age value of thinly to moderately marbled mantle ($<100 \text{ m}$). Thick refractory lumps are not expected to contribute to the He measured in MORB, nor are their $^3\text{He}/^4\text{He}$ ratios anticipated to be affected by ridge activity. Unusually low $^3\text{He}/^4\text{He}$ ratios are observed in MORB along the ultraslow-spreading Southwest Indian Ridge (25), where the crust is unusually thin (26). I suggest that the low $^3\text{He}/^4\text{He}$ ratios simply result from a lesser contribution of the thickest refractory layers to the magmatic He.

The presence of solar (high- $^{20}\text{Ne}/^{22}\text{Ne}$) neon in oceanic basalts (27) can be explained by the same rogue component. Neon diffusivity in olivine is unknown, but Ne and He diffusivities in quartz are identical at 1460°C (28), which justifies the assumption that at high temperatures, the diffusion coefficients of these two gases may be comparable in mantle minerals. As for primordial ^3He , the presence of solar neon in MORB is not expected from a severely degassed mantle reservoir unless it also is held back during melting. More than any other argument, the correlation between $^3\text{He}/^4\text{He}$ and $^{21}\text{Ne}/^{22}\text{Ne}$ ratios in OIB (29) and MORB (30) implies that a primordial component is present in the mantle and that diffusion out of the refractory reservoir is incapable of efficiently separating Ne from He. The similarity of rare gas diffusivities simply reflects that the crossover temperature of Arrhenius plots predicted by the Meyer-Neldel-Winchell compensation law for diffusion falls in the range of mantle temperatures. The isotopic abundances of oxygen and lithophile radiogenic nuclides (^{87}Sr , ^{143}Nd , ^{176}Hf , ^{206}Pb , etc.) in oceanic basalts attest to a complex history and cannot be reconciled with a primordial holding tank of rare gases that would have escaped melting processes. In contrast to He, which does not accumulate in the atmosphere, and to Ne, whose radiogenic ingrowth is slow, Ar is perfectly accounted for by a binary mixture of atmospheric and radiogenic sources, and does not lend itself to a breakdown of separate mantle components.

The present interpretation of mantle He isotope geochemistry turns the rationale behind the canonical model upside down. It views high $^3\text{He}/^4\text{He}$ ratios as attesting to the presence of recycled refractory residues rather than to that of primordial fertile mantle. The refolded parts of the mantle are weak and intensely stretched by mantle flow, and they must be quickly depleted in ^3He by repeated melting events. In contrast, thicker layers of residual material constitute a resistant reservoir for helium with a high $^3\text{He}/^4\text{He}$ ratio: Whichever process removed the fertile constituents from such rocks in the first place (ridge activity, accumulation from an early magma ocean) should have also removed most of their water, making them particularly rigid and resistant to further stretching by mantle convection (31). Old fragments of oceanic lithosphere and refractory cumulates from the magma ocean, rather than

primordial mantle “nuggets,” should host most of the primordial He and Ne observed today in oceanic basalts. Helium with high $^3\text{He}/^4\text{He}$ ratios may contain a component of primordial origin but may not necessarily reflect the reservoir in which it has been residing for most of Earth’s history.

References and Notes

1. S. W. Parman, M. D. Kurz, S. R. Hart, T. L. Grove, *Nature* **437**, 1140 (2005).
2. D. Graham, J. Lupton, F. Albarède, M. Condomines, *Nature* **347**, 545 (1990).
3. H. Craig, J. E. Lupton, *Earth Planet. Sci. Lett.* **31**, 369 (1976).
4. I. Kaneoka, N. Takaoka, *Science* **208**, 1366 (1980).
5. C. J. Allegre, T. Staudacher, P. Sarda, M. Kurz, *Nature* **303**, 762 (1983).
6. D. W. Graham, *Rev. Mineral. Geochem.* **47**, 247 (2002).
7. I. Kaneoka, *Nature* **302**, 698 (1983).
8. M. D. Kurz, W. J. Jenkins, S. R. Hart, *Nature* **297**, 43 (1982).
9. R. K. O’Nions, L. N. Tolstikhin, *Earth Planet. Sci. Lett.* **139**, 213 (1996).
10. C. J. Allegre, *Earth Planet. Sci. Lett.* **150**, 1 (1997).
11. J. C. Lassiter, E. H. Hauri, *Earth Planet. Sci. Lett.* **164**, 483 (1998).
12. J. Blichert-Toft, F. A. Frey, F. Albarède, *Science* **285**, 879 (1999).
13. T. W. Becker, J. B. Kellogg, R. J. O’Connell, *Earth Planet. Sci. Lett.* **171**, 351 (1999).
14. P. J. Wyllie, W. L. Huang, *Contrib. Mineral. Petrol.* **54**, 79 (1976).
15. C. B. Agee, J. Li, M. C. Shannon, S. Circone, *J. Geophys. Res.* **100**, 17 (1995).
16. E. Ohtani, T. Kato, H. Sawamoto, *Nature* **322**, 352 (1986).
17. P. B. Kelemen, N. Shimizu, V. J. M. Salters, *Nature* **375**, 747 (1995).
18. R. M. Ellam, F. M. Stuart, *Earth Planet. Sci. Lett.* **228**, 511 (2004).
19. D. L. Anderson, *Proc. Natl. Acad. Sci. U.S.A.* **95**, 9087 (1998).
20. D. L. Shuster, K. A. Farley, J. M. Sosterson, D. S. Burnett, *Earth Planet. Sci. Lett.* **217**, 19 (2004).
21. C. J. Allegre, D. L. Turcotte, *Nature* **323**, 123 (1986).
22. S. W. Parman, *Nature* **446**, 900 (2007).
23. D. R. Hilton, K. Gronvold, C. G. Macpherson, P. R. Castillo, *Earth Planet. Sci. Lett.* **173**, 53 (1999).
24. D. W. Graham, J. Blichert-Toft, C. J. Russo, K. H. Rubin, F. Albarède, *Nature* **440**, 199 (2006).
25. J. E. Georgan, M. D. Kurz, H. J. B. Dick, J. Lin, *Earth Planet. Sci. Lett.* **206**, 509 (2003).
26. T. A. Minshull, R. S. White, *Geophys. J. Int.* **125**, 139 (1996).
27. M. Honda, I. McDougall, D. B. Patterson, A. Doulgeris, D. Clague, *Earth Planet. Sci. Lett.* **349**, 149 (1991).
28. D. L. Shuster, K. A. Farley, *Geochim. Cosmochim. Acta* **69**, 2349 (2005).
29. M. Honda, I. McDougall, D. Patterson, *Lithos* **30**, 257 (1993).
30. M. D. Kurz et al., *Earth Planet. Sci. Lett.* **232**, 125 (2005).
31. G. Hirth, D. L. Kohlstedt, *Earth Planet. Sci. Lett.* **144**, 93 (1996).
32. The idea defended in this manuscript appeared during discussions with I. Kaneoka while the author was a visiting professor at the Earthquake Research Institute of Tokyo. I thank D. Shuster for sharing helpful information on his diffusion data, and J. Blichert-Toft, D. Graham, and S. Parman for reviewing the manuscript.

4 September 2007; accepted 7 January 2008
Published online 17 January 2008;
10.1126/science.1150060
Include this information when citing this paper.